

Virtual Screening of 4-Anilinoquinazoline Analogues as EGFR Kinase Inhibitors: Importance of Hydrogen Bonds in the Evaluation of Poses and Scoring Functions

V. Aparna,[†] G. Rambabu,[‡] S. K. Panigrahi,[†] J. A. R. P. Sarma,^{*,‡} and G. R. Desiraju^{*,†}

School of Chemistry, University of Hyderabad, Hyderabad 500 046, India, and Informatics Division, GVK BIOSCIENCES Private Limited, 6-3-1192, Begumpet, Hyderabad 500 016, India

Received October 22, 2004

Virtual Screening (VS) is a computational technique that allows selection and ranking of possible hits from a library of compounds. We have carried out VS on 128 selected EGFR kinase inhibitors with GOLD and LigandFit. From the experimental crystal structure of the erlotinib–EGFR complex, three key hydrogen bonds were identified as responsible for anchoring the ligand in the active site. These are of the N–H···N, O_w–H···N, and C–H···O types. Failure to include the hydrogen-bonded water molecule that forms the O_w–H···N bond leads to incorrect results. Of the three interactions, the C–H···O formed by an activated C–H group is the best conserved. On the basis of the efficacy of these hydrogen bonds, the poses were classified into one of three categories: close, shifted, and misoriented. In the VS context, all three interactions need to be modeled correctly so that correct poses and affinities are obtained, and this happens in ligands of the close variety. Cross scoring wherein the poses from one software are input into another for scoring and consensus scoring wherein the scores from various software packages are weighted are also helpful in obtaining better agreements.

INTRODUCTION

Epidermal growth factor receptor (EGFR), in normal physiology, is activated by binding to its cognate ligands, epidermal growth factor, or transforming growth factor alpha (TGF- α) at the extracellular domain causing receptor dimerization, which leads in turn to activation of the intracellular kinase domain.¹ This triggers a cascade of signal transduction events responsible for regulation of cell proliferation. However, EGFR is frequently overexpressed, amplified, and/or mutated in many human solid tumors including breast, ovarian, lung, and squamous cell cancers.² It has also been shown to affect proliferation, angiogenesis, and cancer metastasis.³ Thus, it is being pursued as a molecular target for the treatment of selective cancers.⁴

Drugs targeting EGFR fall into three main categories depending on the receptor region targeted: extracellular, intracellular, and nuclear.⁵ Small molecule inhibitors that target the intracellular EGFR appear to be the most promising approach toward treating EGFR-mediated cancers.⁶ These molecules act by binding either reversibly or irreversibly to the C-terminal tyrosine kinase domain of EGFR, thereby inhibiting autophosphorylation of the receptor and therefore activation. Anilinoquinazolines are the most developed class of drugs that inhibit EGFR kinase intracellularly. These compounds are being studied actively by many research groups,^{7–9} and drug candidates in this class have already reached various phases of clinical trials.

To date, there have been many lead generation and optimization studies reported for this receptor.^{6,7} Also, the

availability of the crystal structure of EGFR complexed with an inhibitor (erlotinib)¹⁰ facilitates the structure-based design of inhibitors against this target. An abundance of relevant literature makes this target suitable for virtual screening (VS).^{10,11} In the present study, we attempt VS of a number of ligands on EGFR kinase and evaluate how different ligand poses fare with respect to the scoring functions.

VS, especially in the context of docking methodologies, is an evolving challenge and an attractive research proposition.¹² It needs to be studied in depth and transformed into a tool of greater confidence and utility. VS consists of two parts, namely, the accurate prediction of pose and the estimation of tightness of binding (scoring).¹³ These two stages are not totally independent, but are linked implicitly through the force field. Still, studies that seek to compare computational techniques for docking have identified that some approaches are good at predicting poses while others are good at computing scores.^{14–16} Therefore, arriving at the appropriate docking/scoring combination is still a challenge.¹⁷ Our goal was to arrive at the best combination of docking and scoring for the EGFR target and to develop a robust VS model. Since both these operations (docking and scoring) would stand to benefit from a better understanding of the ligand–receptor recognition in terms of intermolecular interactions, the major aim of this work is to provide a chemical model that may be used to improve the efficiency of the overall computational effort.

METHODS

Generation of Ligand and Enzyme Structures. The crystal structure of EGFR kinase domain with its bound inhibitor erlotinib {[6,7-bis(2-methoxy-ethoxy)quinazoline-4-yl]-(3-ethynylphenyl)amine} was taken from the Protein Data Bank (PDB entry 1M17).¹⁰ All H-atoms were included. All five water molecules in the active site were included;

* Authors to whom correspondence should be addressed. (G.R.D) tel: +91-40-23134828; fax: +91-40-23010567; e-mail: gautam_desiraju@yahoo.com. (J.A.R.P.S.) tel: +91-40-55259990; fax: +91-40-55626885; e-mail: sarma@gvkbio.com.

[†] University of Hyderabad.

[‡] GVK BIOSCIENCES Private Limited.

Table 1. Structures of 128 EGFR Kinase Inhibitors in the Study

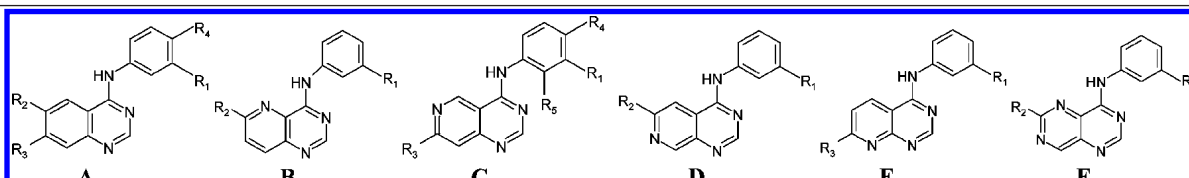
							
Molecule No.	Class	Substitution					Activity pIC ₅₀
		R ₁	R ₂	R ₃	R ₄	R ₅	
1	A	-	-	-	-	-	6.46
2	A	Me	-	-	-	-	6.04
3	A	Cl	-	-	-	-	7.63
4	A	Br	-	-	-	-	7.56
5	A	I	-	-	-	-	7.09
6	A	CF ₃	-	-	-	-	6.23
7	A	Br	NO ₂	-	-	-	6.04
8	A	Br	OMe	-	-	-	6.45
9	A	Br	-	NO ₂	-	-	6.0
10	A	Br	-	OMe	-	-	8.0
11	A	Br	OH	OH	-	-	9.76
12	A	Br	NH ₂	NH ₂	-	-	9.92
13	A	F	-	-	-	-	7.25
14	A	-	OMe	-	-	-	7.25
15	A	-	NH ₂	-	-	-	6.11
16	A	CF ₃	NH ₂	-	-	-	6.24
17	A	-	OMe	-	-	-	6.92
18	A	-	-	NH ₂	-	-	7.0
19	A	CF ₃	-	NH ₂	-	-	8.48
20	A	F	-	NO ₂	-	-	5.21
21	A	Cl	-	NO ₂	-	-	6.09
22	A	I	-	NO ₂	-	-	6.26
23	A	-	OMe	OMe	-	-	7.53
24	A	F	OMe	OMe	-	-	8.42
25	A	Cl	OMe	OMe	-	-	9.5
26	A	I	OMe	OMe	-	-	9.05
27	A	CF ₃	OMe	OMe	-	-	9.61
28	A	Br	NHMe	-	-	-	8.39
29	A	Br	NMe ₂	-	-	-	7.07

Table 1. (Continued)

Molecule No.	Class	Substitution					Activity pIC ₅₀
		R ₁	R ₂	R ₃	R ₄	R ₅	
30	A	Br	NHCOOMe	-	-	-	7.92
31	A	Br	-	OH	-	-	8.32
32	A	Br	-	NHAc	-	-	7.39
33	A	Br	-	NHMe	-	-	8.15
34	A	Br	-	NHEt	-	-	7.92
35	A	Br	-	NMe ₂	-	-	7.95
36	A	Br	NH ₂	NHMe	-	-	9.16
37	A	Br	NH ₂	NMe ₂	-	-	6.79
38	A	Br	NH ₂	OMe	-	-	8.42
39	A	Br	NH ₂	Cl	-	-	8.18
40	A	Br	NO ₂	NHMe	-	-	7.16
41	A	Br	NO ₂	OMe	-	-	7.82
42	A	Br	NO ₂	Cl	-	-	7.6
43	A	Br	OEt	OEt	-	-	11.22
44	A	Br	O-n-Pr	O-n-Pr	-	-	9.76
45	A	H	OMe	OMe	Br	-	10.14
46	B	Br	-	-	-	-	7.46
47	B	Br	NH ₂	-	-	-	8.11
48	B	Br	Cl	-	-	-	7.74
49	B	Br	F	-	-	-	7.35
50	B	Br	NHMe	-	-	-	8.5
51	B	Br	NMe ₂	-	-	-	8.01
52	B	Br	OMe	-	-	-	8.36
53	C	Br	-	-	-	-	7.45
54	C	Br	-	NHAc	-	-	7.53
55	C	Br	-	F	-	-	7.88
56	C	Br	-	OMe	-	-	7.40
57	C	-	-	NH ₂	-	-	6.60
58	C	NO ₂	-	NH ₂	-	-	7.39
59	C	-	-	NH ₂	-	Br	6.61
60	C	Br	-	NH ₂	-	-	8.00
61	C	-	-	NH ₂	Br	-	7.59
62	C	-	-	NH ₂	CF ₃	-	5.32

Table 1 (Continued)


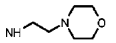
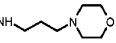
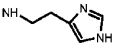
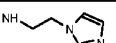
Molecule No.	Class	Substitution					Activity pIC ₅₀
		R ₁	R ₂	R ₃	R ₄	R ₅	
63	C	-	-	NH ₂	-	OMe	5.43
64	C	OMe	-	NH ₂	-	-	6.88
65	C	-	-	NH ₂	OMe	-	6.17
66	C	-	-	NH ₂	-	NH ₂	5.27
67	C	NMe ₂	-	NH ₂	-	-	5.74
68	C	-	-	NH ₂	NMe ₂	-	5.31
69	C	F	-	NH ₂	-	-	6.07
70	C	Cl	-	NH ₂	-	-	6.92
71	C	OH	-	NH ₂	-	-	7.15
72	C	Me	-	NH ₂	-	-	7.39
73	D	Br	-	-	-	-	7.29
74	D	Br	Cl	-	-	-	7.39
75	D	Br	F	-	-	-	6.9
76	D	Br	OMe	-	-	-	8.58
77	D	Br		-	-	-	8.63
78	E	Br	-	-	-	-	6.16
79	E	Br	-	NH ₂	-	-	6.02
80	E	Br	-	F	-	-	6.16
81	E	Br	-	NHMe	-	-	7.28
82	E	Br	-	NMe ₂	-	-	6.48
83	E	Br	-	OMe	-	-	6.58
84	F	H	NHMe	-	-	-	7.88
85	F	Br	Cl	-	-	-	7.08
86	F	Br	NH ₂	-	-	-	8.82
87	F	Br	NHMe	-	-	-	9.11
88	F	Br	NMe ₂	-	-	-	9.02
89	F	Br	OMe	-	-	-	8.42
90	F	Br		-	-	-	9.09
91	F	Br		-	-	-	8.53
92	F	Br		-	-	-	9.6
93	F	Br		-	-	-	8.63

Table 1 (Continued)

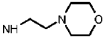
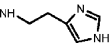
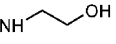
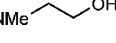
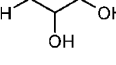
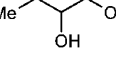
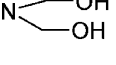
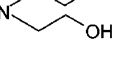
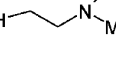
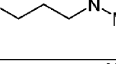
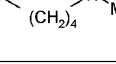
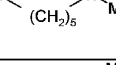
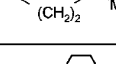
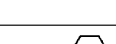
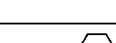
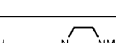
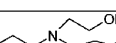
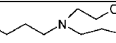

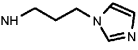
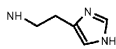
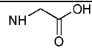

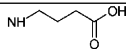
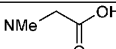
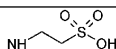
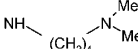
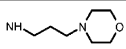
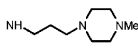
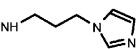
Molecule No.	Class	Substitution					Activity pIC ₅₀
		R ₁	R ₂	R ₃	R ₄	R ₅	
94	F	Me	Cl	-	-	-	6.42
95	F	Me	NH ₂	-	-	-	7.76
96	F	Me	NHMe	-	-	-	8.36
97	F	Me	NMe ₂	-	-	-	8.39
98	F	Me		-	-	-	8.63
99	F	Me		-	-	-	8.52
100	C	Br	-		-	-	9.61
101	C	Br	-		-	-	8.58
102	C	Br	-		-	-	9.03
103	C	Br	-		-	-	8.49
104	C	Br	-		-	-	7.85
105	C	Br	-		-	-	7.92
106	C	Br	-		-	-	7.34
107	C	Br	-		-	-	8.05
108	C	Br	-		-	-	8.13
109	C	Br	-		-	-	8.07
110	C	Br	-		-	-	7.39
111	C	Br	-		-	-	8.49
112	C	Br	-		-	-	8.72
113	C	Br	-		-	-	8.26
114	C	Br	-		-	-	8.30
115	C	Br	-		-	-	8.03
116	C	Br	-		-	-	8.92

Table 1 (Continued)

Molecule No.	Class	Substitution					Activity pIC ₅₀
		R ₁	R ₂	R ₃	R ₄	R ₅	
117	C	Br	-	NHNH ₂	-	-	8.14
118	C	Br	-		-	-	9.29
119	C	Br	-		-	-	9.04
120	C	Br	-		-	-	8.82
121	C	Br	-		-	-	9.21
122	C	Br	-		-	-	9.55
123	C	Br	-		-	-	7.79
124	C	Br	-		-	-	8.85
125	C	Me	-		-	-	8.26
126	C	Me	-		-	-	8.03
127	C	Me	-		-	-	8.25
128	C	Me	-		-	-	8.45

the acidic and basic residues in the active site are in the ionic form. The protein was subjected to minimization using steepest descent (gradient <0.1) and conjugate gradient algorithms (gradient <0.01) using the CHARMM force field in InsightII.¹⁸ The active site was defined as consisting of all amino acids within a 15 Å radius from the center of the ligand.¹⁹ The tautomeric states of two histidines, His781 and His811, which are in the active site were set to the N_δ form. However, they are too far from the ligand (>12 Å) to have any real impact in the docking studies.

A set of 128 4-anilinoquinazoline analogues reported to inhibit EGFR kinase was compiled by us earlier.²⁰ These ligands have six slightly varying skeletons (Table 1) and originate from different reports.^{21–26} They include simple quinazolines (class A: 45 compounds), pyrido[3,2-*d*]pyrimidines (B: 7 compounds), pyrido[4,3-*d*]pyrimidines (C: 49 compounds), pyrido[3,4-*d*]pyrimidines (D: 5 compounds), pyrido[2,3-*d*]pyrimidines (E: 6 compounds), and pyrimido[5,4-*d*]pyrimidines (F: 16 compounds). The biological activities were converted into the corresponding pIC₅₀ values. All the IC₅₀ values had been obtained using the same assay method.²⁷

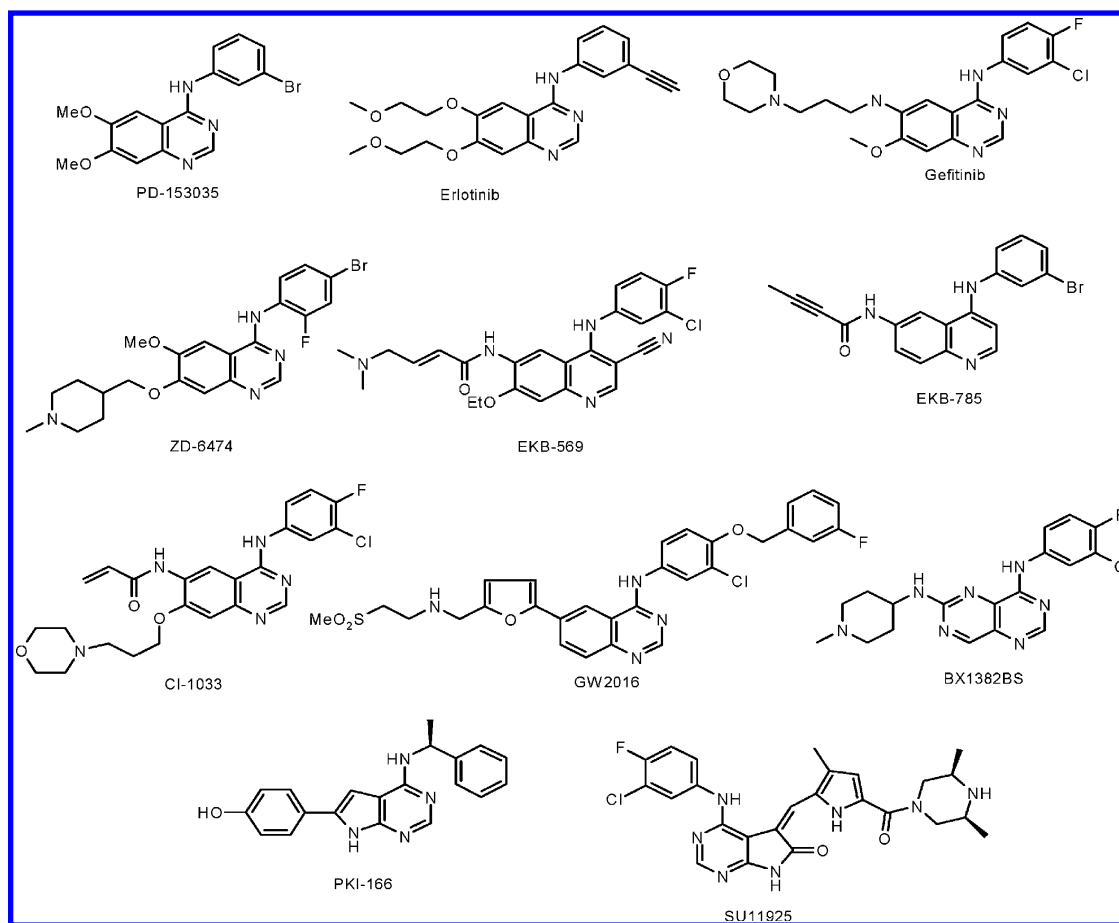
All ligand structures were built in Cerius²⁸ and minimized by OFF methods using the steepest descent algorithm with a gradient convergence value of 0.001 kcal/mol. Partial

atomic charges were calculated using the Gasteiger method. Further geometry optimization was carried out for each compound with the MOPAC 6 package using the semiempirical AM1 Hamiltonian. The resulting geometries with partial charges were used for further calculations.

Docking. GOLD.²⁹ We used the standard set parameters in all the calculations. For each of the 10 independent Genetic Algorithm (GA) runs, with a selection pressure 1.1, 100 000 GA operations were performed on a set of five islands with a population size of 100 individuals. Default operator weights were used for crossover, mutation, and migration of 95, 95, and 10, respectively. Default cutoff values of 2.5 Å for hydrogen bonds and 4.0 Å for vdW were employed. To further speed up the calculation, the GA docking was stopped when the top three solutions were within 1.5 Å RMSD of each other. All other values were set to the default. GOLD and Chem-scores were calculated. While docking, a limited flexibility is allowed for the hydrogen atoms in the -OH and -NH₃ substituents of the side chains of Ser, Thr, and Lys residues.

LigandFit.³⁰ Docking was performed with Monte Carlo simulations using the CFF95 force field. Two different simulations were performed with 20 000 and 99 999 iterations. The electrostatic energy was included. A grid resolution was set to 0.5 Å (default), and the ligand-accessible grid

Scheme 1



was defined such that the minimum distance between a grid point and the protein is 2.0 Å for hydrogen and 2.5 Å for heavy atoms. The grid extends from the defined active site to a distance of 3 Å in all directions. This grid was used to calculate the nonbonded interactions between all the atoms of ligands and protein residues. Nonbonded cutoffs were set to 10 Å while using a distance-dependent dielectric constant. After every iteration, 10 iterations of minimization were performed before being considered in the next iteration, and the selected configuration was minimized for 100 iterations. Flexible fit, wherein the ligand conformational space is explored with different initial poses, was selected in the Monte Carlo simulations. To avoid identical conformations, an RMSD cutoff of 1.5 and a score cutoff of 20 kcal mol⁻¹ were maintained while saving the final conformations. The top 20 conformations were saved after rigid body minimizations of 1000 steps. Dockscore, Ligscore1 and Ligscore2, LUDI, PMF, PLP1 and PLP2, JAIN, H-bonding, and vdW scores were calculated for each of the 20 saved ligand conformations.

RESULTS AND DISCUSSION

EGFR is one of the few thoroughly studied and well-validated targets in anti-cancer therapy.⁴ To pursue VS of EGFR, the choice of 128 ligands was based on the following criteria:

1. The compounds must have good structural diversity, and binding studies should have been carried out by the same biological assay.
2. Ideally, the same group should have reported the activities at the same time or over a short period of time without much variation in the assay technique.

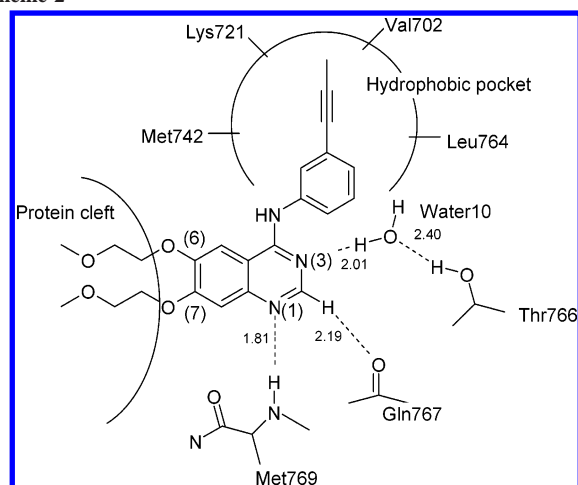
3. Structural similarity with erlotinib (in the crystal structure) should be present. This enables one to evaluate the RMSD of the poses with that of the experimental structure.

It is pertinent to state that our choice of 128 ligands is validated by the structures of many drugs currently in clinical trials or even marketed. For example, the following may be mentioned: PD-153035, erlotinib (Traceva, CP-358774, OSI-774), gefitinib (Iressa, ZD-1839), ZD-6474, EKB-569, EKB-785 (CL-387785), canertinib (CI-1033, PD-183805), GW-2016 (GW-572016), and BX-1382BS are all based on the basic anilinoquinazoline scaffold, while PKI-166 and SU11925 have a five-membered ring (rather than a six-membered ring) fused to the 4-aminopyrimidine unit (Scheme 1).³¹

Direct Docking. The main objective of the present work is to perform a docking analysis of selected EGFR kinase inhibitors. GOLD being widely regarded as one of the best docking programs,^{12,14,32} our initial studies were carried out with this software. Initially, the docking studies were carried out on the protein molecule without any crystallographically observed water molecules. These studies resulted in poor docking of ligands in the active site and accordingly in poor correlation between the GOLD scores and activities. On careful analysis of 1M17 and other kinase crystal structures, it was observed that one or a few water molecules participate effectively in ligand–receptor interactions.¹⁰ Scheme 2 shows the hydrogen bond and hydrophobic environment around the ligand in 1M17.

The N(3) of the pyrimidine ring accepts an O_w–H...N hydrogen bond from a water molecule (water10), which in turn forms a cooperative O–H...O_w H-bond involving Thr766

Scheme 2



of the protein.³³ In direct docking, initially the water molecules are not considered, and so these crucial hydrogen bonds are not included. Therefore, docking is not effective, and there is little to no correlation between the scores and the observed activities. Accordingly, a conscious decision was made to include not only this water molecule but also four other water molecules¹⁹ that have been observed in the erlotinib–EGFR crystal structure. These water molecules have been considered as a part of the inflexible protein molecule in the docking studies. The four other water molecules are not near the ligand and will not be discussed further. After including the five water molecules, an improvement was observed, but the correlation between the observed activity and the scores was still disappointing (Figure 1).

Cross Docking. The scatterplot of scores obtained from each of these methods against the activity (pIC_{50}) of the ligands is shown in Figure 1. GOLD seems to be slightly better than the LigandFit. When LigandFit was used with only 20 000 Monte Carlo iterations, the nonbonded energies for most of the ligands were positive (Supporting Information), and the results were unacceptable. When the docking was rerun with a maximum number of iterations (99 999), there was a slight improvement, but the data were still too scattered with little to no correlation (Figure 1). LigandFit is better in the high range but is poor in predicting low and medium active compounds. There are too many false positives and false negatives. GOLD is somewhat better for low

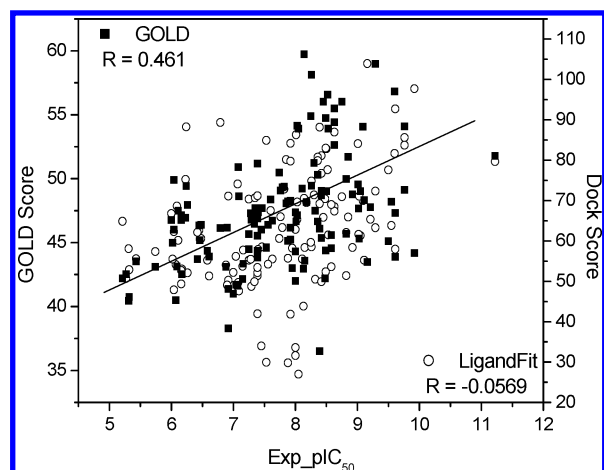


Figure 1. Scatterplot of GOLDScore and Dockscore (with 99 999 Monte Carlo simulations) vs activity.

and medium active compounds but does not seem to fare well with high actives, again producing false positives and negatives. We concluded that the problem could lie either in the prediction of poses and/or in the computation of the scores.

Pose Analysis with RMSD. Which program docks the ligand better and identifies the bioactive conformation more accurately? To answer this question we examined erlotinib (Figure 2a, Scheme 2). In addition to the hydrogen bonds mediated by water discussed above, there are two other significant hydrogen bonds. The N(1) of quinazoline ring accepts a $\text{N}-\text{H}\cdots\text{N}$ bond from the backbone $\text{N}-\text{H}$ of Met769, and there is a good $\text{C}-\text{H}\cdots\text{O}$ hydrogen bond formed between the activated C(2)-H group and the backbone carbonyl oxygen of Gln767.³⁴

In effect, these three hydrogen bonds, which are roughly worth around $3-5 \text{ kcal mol}^{-1}$ each (between 10 and 15 kcal mol^{-1} collectively, or roughly a quarter of the total binding enthalpy), anchor the ligand in the active site. This particular energy range for an individual hydrogen bond is termed “weak” in the literature, and the term is used here with no additional connotations.³⁵ Additionally, the 6- and 7-substituents project outside the active site (actually, in the cleft region between the C-terminal and N-terminal lobes), and the meta-substituted 4-anilino group fits well in the Thr766–Leu764–Met742–Lys721–Val702 hydrophobic pocket. In effect, these weak hydrogen bonds provide a template effect (chemical recognition), but further activity depends on the insertion of the 4-anilino ring into the hydrophobic pocket (geometrical recognition).

To evaluate the capabilities of the various programs to model these hydrogen bonds, erlotinib was docked using each of the two programs, and the relative orientations of the ligand are shown in Figure 2b.

The RMSDs were calculated on the basis of the 4-anilinoquinazoline fragment (Scheme 3). Although LigandFit predicted the orientation correctly, it displaced the molecule significantly. GOLD performed better with a pose with the minimum RMSD. In this respect, these programs were able to reproduce the hydrogen bond arrangement of the experimental crystal structure. Accordingly, we generated RMSDs for the 128 molecules in the study for both GOLD and LigandFit poses (Supporting Information). A scatterplot of these RMSD values versus experimental pIC_{50} values is shown in Figure 3.

The performance of the two programs in docking the molecules in the active site is analyzed in term of RMSD and is summarized in Table 2. On the basis of the RMSDs alone, it would appear that GOLD and LigandFit are comparable, or perhaps one could state that GOLD performs slightly better in that 118 out of 128 molecules have $\text{RMSD} < 1.0 \text{ \AA}$ while LigandFit has 34 molecules with $> 1.0 \text{ \AA}$ RMSD.

Pose Analysis with Intermolecular Interactions. A second type of analysis was carried out to further discriminate between GOLD and LigandFit in the prediction of correct poses. Interaction-based evaluation of the generated poses may add more meaning to the measurement of docking accuracy as compared to the normal RMSD based classifications.³² The best poses for the ligands were analyzed in terms of the three key hydrogen bonds mentioned above. For a full list of hydrogen bond metrics, see the Supporting Information. On the basis of the efficacy of these interactions, the poses were classified into one of three categories: name-

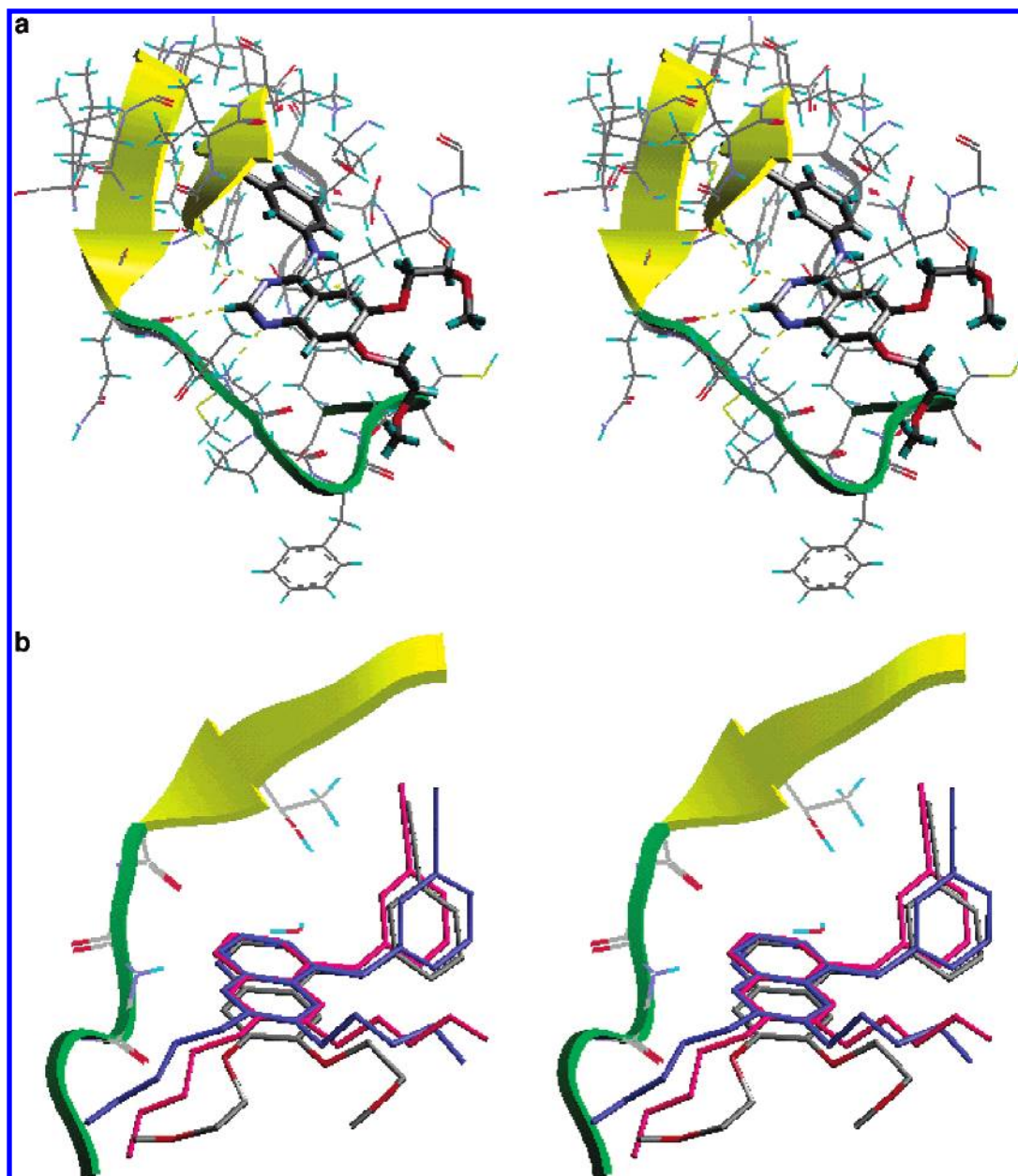


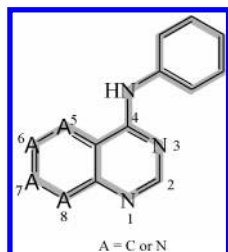
Figure 2. (a) Stereoview of active site residues and erlotinib ligand in the crystal structure of 1M17. The three hydrogen bonds that lock the heterocyclic ring are shown as dashed lines. For clarity, only some of the active site residues are shown. (b) Overlay picture of erlotinib (experimental) and the docked conformations obtained from GOLD (pink, RMSD: 1.073) and LigandFit (blue; 1.563) in the active site.

ly, close, shifted, and misoriented. A *close* category corresponds to conformations with low RMSD and has all the three crucial hydrogen bonds intact. A *shifted* category refers to conformations that have medium RMSD values and with the ligand translated with respect to the erlotinib position, and naturally some of the hydrogen bonds are missing or distorted. Finally, the *misoriented* category refers to cases where the orientation itself is completely different from that

in erlotinib. Needless to say, all the three hydrogen bonds have disappeared in the misoriented cases. Figure 4 illustrates these three situations.

Table 3 lists the numbers of close, shifted, and misoriented molecules obtained from GOLD and LigandFit. Although the RMSDs of the poses given by LigandFit were nearly comparable to those generated by GOLD (Table 2), visual inspection revealed that all the ligands were completely misoriented! This could be due to two factors: (1) the methodology used to find the correct poses is not good enough so that the “best” pose obtained at the end of the stipulated number of simulations is routinely accepted by the program or (2) the improper or excessive weightage has been given for the vdW interactions with respect to the hydrogen bonds. In GOLD, however, nearly 67% of the ligands are in the close category, while 21% and 12% are in the shifted and misoriented categories, respectively (Sup-

Scheme 3



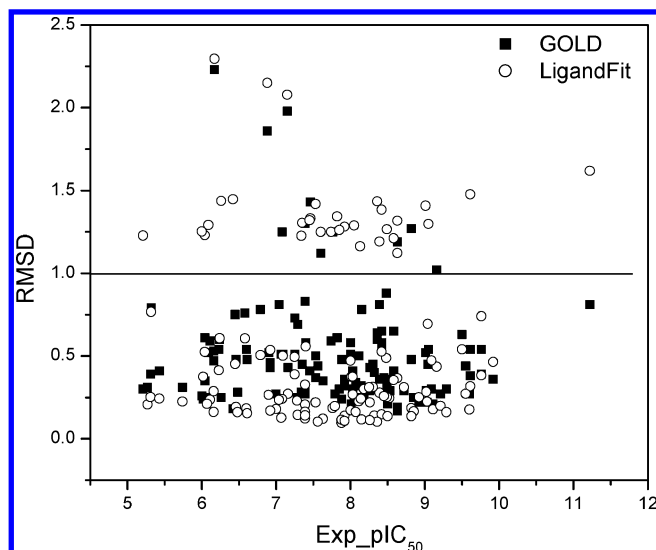


Figure 3. Scatterplot of RMS deviations of docked conformations obtained from GOLD and LigandFit vs activity.

Table 2. Summary of RMS Deviations of Conformations Obtained from GOLD and LigandFit

RMSD	GOLD	LigandFit
≤0.5	86	83
0.5–1.0	32	13
1.0–1.5	7	28
1.5–2.0	2	1
2.0–2.5	1	3

porting Information). Thus, while GOLD certainly outperforms LigandFit in generating good poses, it is still not flawless. Furthermore, these results show the dangers of relying on RMSDs alone.

A further analysis of the three hydrogen bonds is in order. The N–H···N between Met769 and N(1) and the O_w–H···N between water10 and N(3) involve so-called “strong” donors and acceptors, while the C–H···O between Gln767 and C(2)–H is ostensibly weak because a C–H donor is involved. These terms weak and strong reflect an older, classical bias, but according to more modern views, all these hydrogen bonds lie in a continuum between the very weak (~0.25 kcal mol⁻¹) to very strong (~40 kcal mol⁻¹).³⁶ This range spans the gamut between van der Waals interactions and quasi-covalent bonds, but they all share important supramolecular characteristics. In general, we note that the N–H···N is one of the weakest types of hydrogen bonds involving strong donors and acceptors (N, O, halide); we also note that hydrogen bonds with water as donor lie at the border between strong and weak. In the present case, the N–H···N distance (*d*) is 1.81 Å while O_w–H···N is 2.01 Å (Scheme 2). Strikingly, the C–H···O bond involves a donor that is activated by the two flanking heterocyclic nitrogen atoms and is as short as 2.19 Å. Therefore, it is very significant for an interaction that involves a so-called weak donor.³⁷ We estimate that the C–H···O is of the same if not greater significance than the N–H···N and O_w–H···N interactions, in this particular case. All in all, it may be safely said that the three key hydrogen bonds that pin the ligand in the active site are nearly comparable in their overall importance, being nearly equal in distance.³⁸ This means, in the VS context, that all three weak interactions need to be modeled correctly in order that the correct affinity is

obtained. Clearly, this can only happen for ligands in the close category.

In GOLD, all the molecules in this close category interact correctly with the key residues in the immediate vicinity of the ligand, with respect not only to the hydrogen bonds but also to the hydrophobic interactions formed by the 4-anilino group. Figure 5a is a representation of the three hydrogen bonds (*d*–*θ* plot) in the active site. Note the profusion of interactions and also that the number of (C–H···O), (O_w–H···N), and (N–H···N) points is nearly the same. Notably, the C–H···O distribution is the tightest in terms of length (shorter than N–H···N) and angle. This is a clear demonstration of the fact that the C–H···O interaction is the most significant of the three hydrogen bonds. This is true for ligands in all activity ranges.

In the shifted category, the overall hydrogen bond situation is less satisfactory (Figure 5b). The C–H···O interactions are largely conserved, again indicating that they are the most important among the three hydrogen bonds. The O_w–H···N interactions become much shorter and, therefore repulsive, while the N–H···N interactions become longer. Why does this happen? Almost all the ligands in this shifted category have an elongated substituent on C(7) (the converse is not true) and no substituent on C(6). The effect of this is to “push” the ligand closer to water10 and Thr766 leading to an unfavorably short contact. Some compounds showing this behavior are **17–20**, **27**, **44**, **54**, **91**, **102–105**, **108**, **115**, **117–120**, and **127**.³⁹ Concomitantly, the N–H···N interaction elongates. The misoriented category is more drastically in error. For all the molecules in this category, there is hardly any substitution at the 6- or 7-positions. At most, there is a small substituent like fluoro, amino, or nitro at one of these two positions; this is exemplified by ligands **1–8**, **13**, **55**, **73**, **75**, **78**, **80**, and **112**. In effect, the molecule is flipped around to obtain an orientation that is a near-shape mimic (this is why the RMSDs sometimes appear satisfactory for this category). The hydrogen bonds have been given a go-by, and this pose has no chemical or biological significance.

Considering the importance in modeling the hydrogen bonds correctly, we examined all 10 solutions offered by GOLD for the shifted and misoriented cases, in particular to ascertain if there are any with correct hydrogen bond geometry even if the affinity was not modeled properly. The aim of this exercise was to identify solutions with the correct pose, for if the pose is incorrect, there is no question of proceeding further. The hope was that if a solution with the correct pose were found (hydrogen bonds modeled correctly), the scores (for that solution) would also be correct. Gratifyingly, for the shifted category, 23 out of 27 ligands had other solutions with correct poses.⁴⁰ For the misoriented category, however, there was no solution, as might have been expected. The scores for the 23 (improved) ligands in the shifted category and all the ligands in the close category were analyzed (Figure 6). Although there is an improvement in the correlation, it is not significant enough, and there are still a number of false positives and false negatives. Therefore, one is led to the inescapable feeling that these disagreements arise from the lack of C–H···O and other hydrogen bond parametrization. Further absence of electrostatic terms may also affect the Fitness function (GOLDScore). Some of these interactions play a crucial role in locking the molecule in the active site and also contribute significantly in the scores.

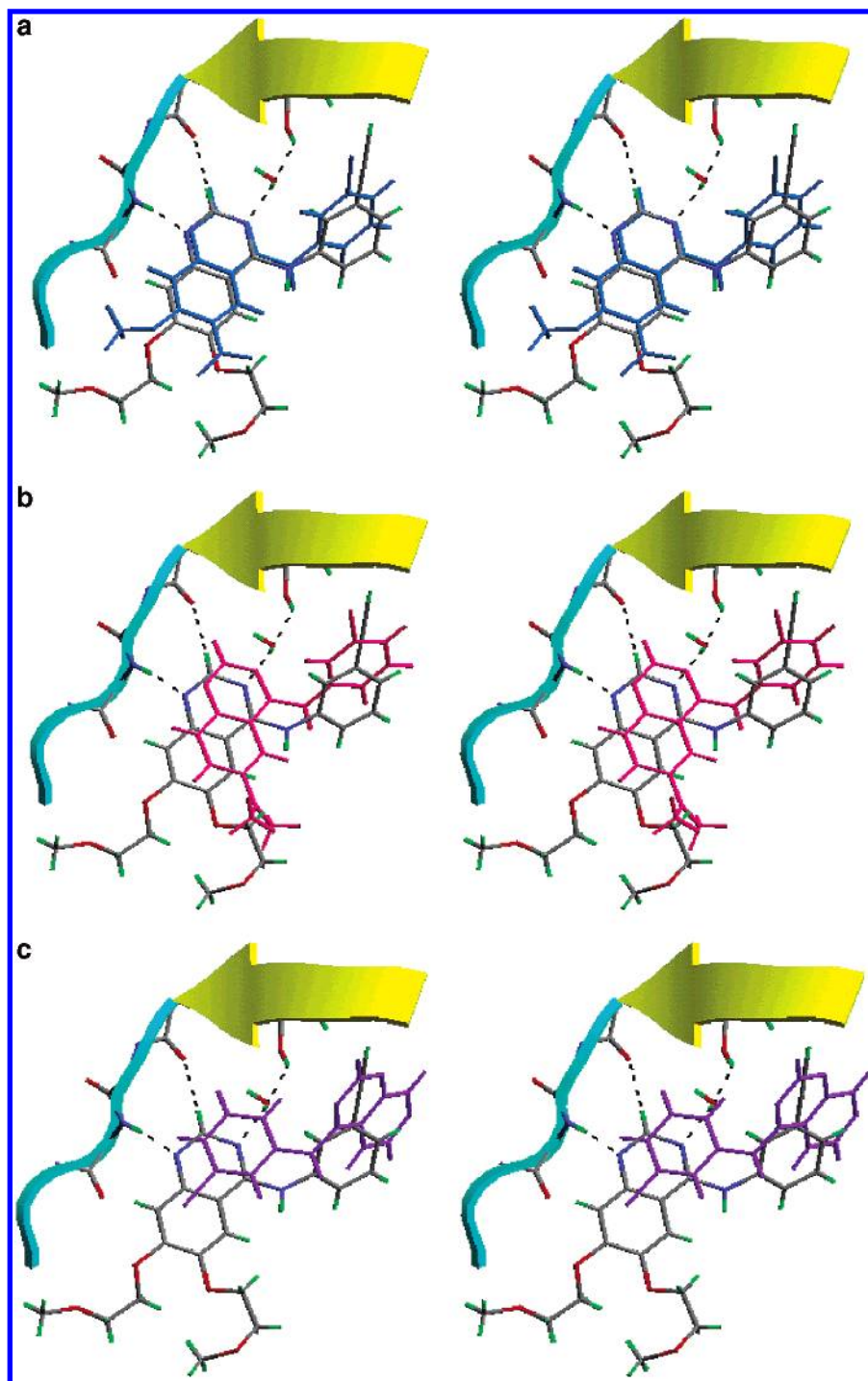


Figure 4. (a) Stereoview of a close category ligand, **25** (blue). Erlotinib is also shown. (b) Stereoview of a shifted category ligand, **108** (pink), shown with erlotinib. (c) Stereoview of a misoriented category ligand, **75** (purple), with erlotinib.

Table 3. Classification of GOLD and LigandFit Poses of Ligands (Active, Medium, Inactive) Based on Alignment of Interactions (Close, Shifted, Misoriented) in the Active Site

	GOLD			LigandFit		
	active ($\text{pIC}_{50} > 8$)	medium ($\text{pIC}_{50} 6-8$)	inactive ($\text{pIC}_{50} < 6$)	active ($\text{pIC}_{50} > 8$)	medium ($\text{pIC}_{50} 6-8$)	inactive ($\text{pIC}_{50} < 6$)
close	42	40	4	1	0	0
shifted	17	7	3	0	3	0
misoriented	0	15	0	58	59	7

Cross Scoring. With the observation that the poses from GOLD were much better and that each software has its own methods to calculate scores, we used these GOLD poses as

inputs to calculate scores such as Dockscore, Ludi, Ligscore, PLP, and PMF in LigandFit. We term this procedure as cross scoring. Thus, the GOLD poses were held rigidly in the ac-

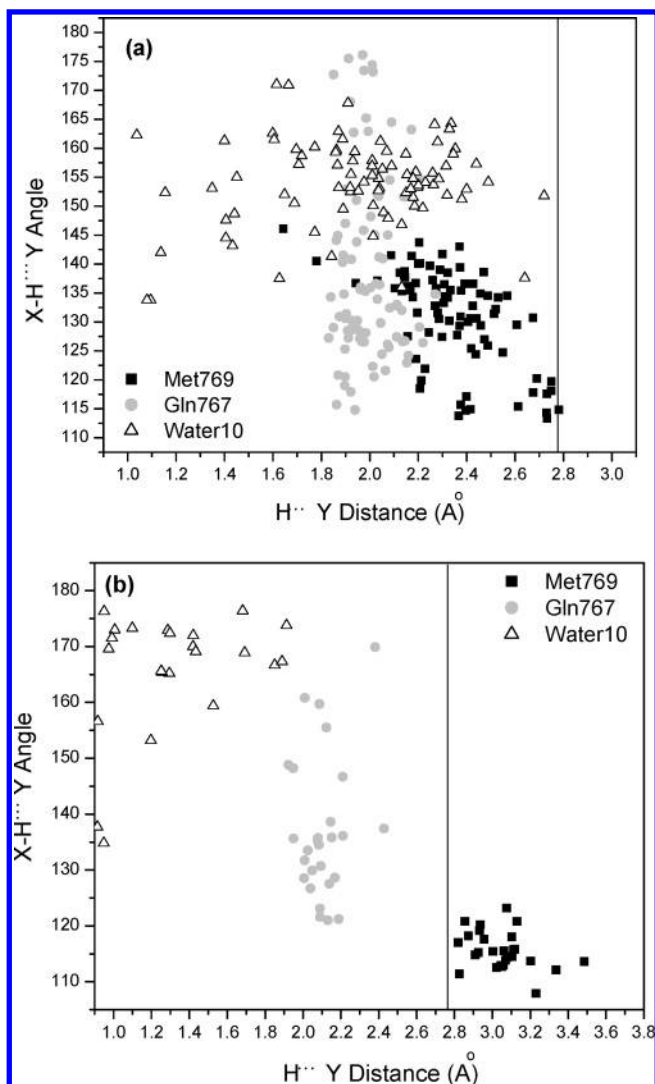


Figure 5. d - θ scatterplot of the three key active site hydrogen bonds in the (a) close category and (b) shifted category. Note that the N-H...N (Met769) interactions have elongated in panel b as compared to panel a, while the O_w-H...N (water10) interactions have shortened unacceptably. The C-H...O (Gln767) interactions are largely conserved in both the cases.

tive site, and the different scores were calculated. The Dockscore of LigandFit produced an improved correlation shown in Figure 7.

It may be noted that, to maintain the GOLD generated pose in LigandFit, care must be taken to explicitly include electrostatic terms and to ignore the "short" distances that in reality correspond to good hydrogen bonds but is taken by the program as corresponding to bad contacts. The correlation was much improved, but the small number of false positives and false negatives is still nagging.

Consensus Model. The results obtained this far are mixed but have several favorable features. First, fully 67% of the ligands belong to the close category in GOLD, meaning that both hydrogen bonds and hydrophobic interactions are being modeled properly in these cases or at least that the program does not consider these short contacts as being repulsive. Second, if the LigandFit is suitably "doctored" by neglecting short distances that are actually true hydrogen bonds, the correlation improves. This doctoring was carried out by a toggle on the switch entitled, "Explicitly Exclude listed H-bonds repulsive terms". To get a better VS model, a

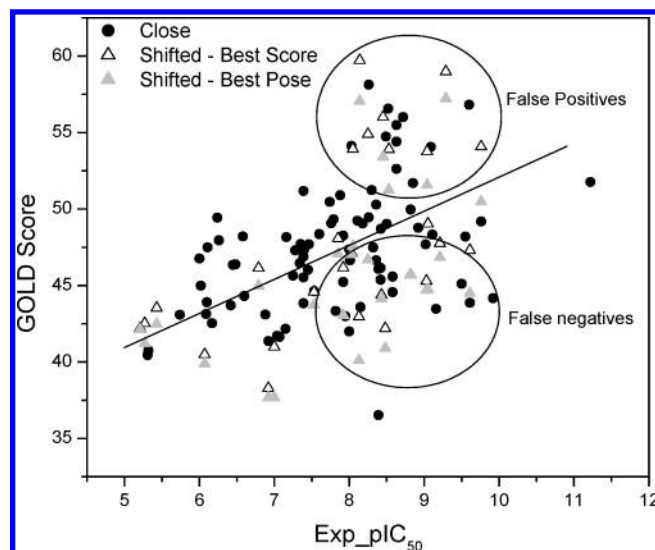


Figure 6. Experimental pIC₅₀ values vs GOLD scores of compounds that have all three key hydrogen bonds between heterocyclic and protein residues and water in the active site. Note that the false positives improve more than the false negatives because of this treatment. Compound 72 (far right) is a common outlier in all the docking studies.

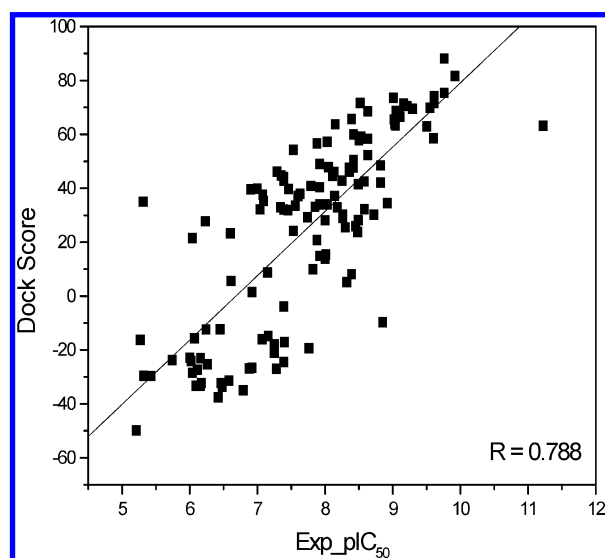


Figure 7. Scatterplot of Dockscore (LigandFit) vs activity obtained after docking GOLD conformations rigidly into the active site.

multiple regression analysis was carried out using 12 different scores (consensus scoring).¹⁵ For each ligand the best solution from GOLD (ligand, protein, and water) was directly read into LigandFit and rescored without any further optimization or changes. All such regenerated scores along with GOLD scores were used in a multivariate analysis to produce a consensus model. Of the 128 ligands, 97 were used in the training set and 31 in the test set. A combination of GOLDScore, Dockscore, Ludiscore, and PLPScore gave a better model than any other (Figure 8) combination of scores.

The final equation generated by this multiple linear regression is given below:

$$\text{activity} = 1.14722 + 0.058516 (\text{GOLDScore}) + 0.21474 (\text{Dockscore}) + 0.003935 (\text{Ludiscore}) - 0.028526 (\text{PLPScore})$$

The coefficient of each term is a measure of the contribution

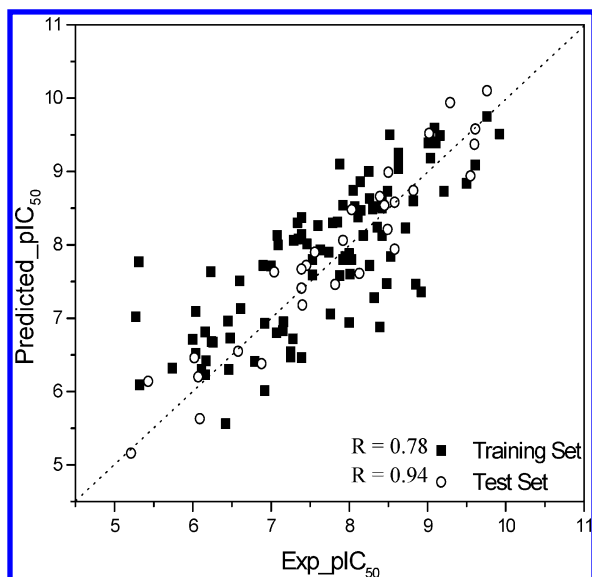


Figure 8. Scatterplot of experimental vs predicted activities using consensus scoring.

of each scoring function toward the final model. It is well-known that Dockscore estimates the hydrophobic interactions correctly. PLP of LigandFit is known to have a high success rate in scoring hydrophobic complexes. The final model ($r^2 = 0.881$, $r^2_{cv} = 0.81$, PRESS = 10.55, $r^2_{bs} = 0.87$) was validated by the test set of 31 molecules.⁴¹ The model was able to correctly predict the activity of 93% of the molecules to within an order of magnitude.

CONCLUSIONS

This study describes VS of a library of 128 EGFR kinase inhibitors. We show that acceptable results may be obtained when the outputs from commercial software packages are analyzed and modified on the basis of a chemical model that incorporates specific hydrogen bonds. We have shown that, for these 4-anilinoquinazoline-type ligands, inclusion of a hydrogen-bonded water molecule at N(3) is indispensable to obtain meaningful VS results. GOLD and LigandFit have variable success in identifying correct poses and binding affinities. We have demonstrated that poses from GOLD are invariably better and that these may be input into the LigandFit to get more accurate results. Consideration of ligand–protein hydrogen bonds of the N–H \cdots N, O $_w$ –H \cdots N, and above all the C–H \cdots O type seems to be very important to obtain accurate poses and binding affinities. The current software does not seem to model these interactions adequately. At best, in the close category, these geometries are not considered excessively repulsive; at worst, in the shifted category, false poses are produced. The misoriented cases are practically meaningless. What one needs is a modification in the software so that these hydrogen bonds are properly searched for among putative inhibitors, in other words these interactions need to be appropriately weighted in the scoring functions. Hydrophobic interactions are also important, but they are nonspecific and lead to an all-or-nothing situation, pertaining as they do to a good fit of the 4-anilino fragment into a hydrophobic pocket of the protein. To summarize, meaningful modeling of the hydrogen bonds, which to a large extent would account for the electrostatics, is necessary but not sufficient for good correlations. Adequate

modeling of both hydrogen bonds and hydrophobic interactions is both necessary and sufficient.

Most pertinently, VS as a technique is supposed to rapidly screen large chemical libraries and to “cherry pick” and rank the few active ones from the very large number of moderately active and inactive compounds—the so-called needle in the haystack problem. Any scientific technique that aims at both speed and accuracy is necessarily difficult to optimize. Till today, VS approaches have concentrated on speed and automation. The present study shows that discrepancies in the screening results may be rationalized on the basis of models that explicitly take into account specific intermolecular interactions. But this is a necessarily subjective and slow activity. At the same time, when appropriate chemical (supramolecular) models are invoked, there seems to be little doubt that the VS results improve. How then does one reconcile these two seemingly incompatible approaches to VS? We suggest that future versions of the software should address chemical issues more directly, especially the presence and role of strong and weak hydrogen bonds, that is particular supramolecular synthons,⁴² in order that VS becomes increasingly accurate and reliable.

ACKNOWLEDGMENT

G.R.D. thanks the DST and CSIR for their continuing financial support to his research programs over the years. J.A.R.P.S. thanks G. V. Sanjay Reddy, CEO GVK BIOSCIENCES Pvt. Ltd., for his support and encouragement and B. S. R. Nagakumar for technical assistance. S.K.P. and V.A. thank the CSIR for the award of a JRF. G.R.D., S.K.P., and V.A. acknowledge with gratitude the Centre for Modelling, Simulation and Design (CMSD) set up in the University of Hyderabad under the UGC program for Universities with Potential for Excellence (UPE). We thank B. Gopalakrishnan (TCS, Hyderabad) for his input and helpful comments throughout this study.

Supporting Information Available: Table of scores and RMSD values of best poses obtained from GOLD, LigandFit, and classification of GOLD poses based on interactions (Table 1). Table of metrics of hydrogen bonds formed by GOLD poses (Table 2). Table of experimental and predicted activities for training and test sets of two consensus models I and II (Table 3). Scatterplot of Dockscore (LigandFit after keeping 20 000 Monte Carlo simulations) versus experimental activity (Figure 1). Scatterplot of experimental versus predicted activities using consensus model II (Figure 2). This material is available free of charge via the Internet at <http://pubs.acs.org>.

REFERENCES AND NOTES

- (1) Yarden, Y. Growth factor receptor tyrosine kinases. *Annu. Rev. Biochem.* **1998**, *57*, 443–478.
- (2) Aaronson, S. A. Growth factors and cancer. *Science* **1991**, *254*, 1146–1152.
- (3) Barnes, C. J.; Kumar, R. Epidermal growth factor receptor family tyrosine kinases as signal integrators and therapeutic targets. *Cancer Metastasis Rev.* **2003**, *22*, 301–307.
- (4) Cohen, P. Protein kinases—the major drug targets of the twenty-first century? *Nat. Rev. Drug Discovery* **2002**, *1*, 309–315.
- (5) Pedersen, M. W.; Poulsen, H. S. Epidermal growth factor receptor in cancer therapy. *Sci. Med.* **2002**, *8*, 206–217.
- (6) Bridges, A. J. Chemical inhibitors of protein kinases. *Chem. Rev.* **2001**, *101*, 2541–2572.
- (7) Traxler, P.; Bold, G.; Buchdunger, E.; Caravatti, G.; Furet, P.; Manley, P.; O'Reilly, T.; Wood, J.; Zimmermann, J. Tyrosine kinase inhibitors: From rational design to clinical trials *Med. Res. Rev.* **2001**, *21*, 499–513.

- (8) Wissner, A.; Overbeek, E.; Reich, M. F.; Floyd, M. B.; Johnson, B. D.; Mamuya, N.; Rosfjord, E. C.; Discafani, C.; Davis, R.; Shi, X.; Rabindran, S. K.; Gruber, B. C.; Ye, F.; Hallett, W. A.; Nilakantan, R.; Shen, R.; Wang, Y.-F.; Greenberger, L. M.; Tsou, H.-R. Synthesis and structure–activity relationships of 6,7-disubstituted 4-anilinoquinoline-3-carbonitriles. The design of an orally active, irreversible inhibitor of the tyrosine kinase activity of the epidermal growth factor receptor (EGFR) and the human epidermal growth factor receptor-2 (HER-2). *J. Med. Chem.* **2003**, *46*, 49–63.
- (9) Smaill, J. B.; Rewcastle, G. W.; Loo, J. A.; Greis, K. D.; Chan, O. H.; Reyner, E. L.; Lipka, E.; Showalter, H. D. H.; Vincent, P. W.; Elliott, W. L.; Denny, W. A. Tyrosine kinase inhibitors. 17. Irreversible inhibitors of the epidermal growth factor receptor: 4-(phenylamino)-quinazoline- and 4-(phenylamino)pyrido[3,2-d]pyrimidine-6-acrylamides bearing additional solubilizing functions. *J. Med. Chem.* **2000**, *43*, 1380–1397.
- (10) Stamos, J.; Silwowski, M. X.; Eigenbrot, C. Structure of the epidermal growth factor receptor kinase domain alone and in the complex with a 4-anilinoquinazoline inhibitor. *J. Biol. Chem.* **2002**, *277*, 46265–46272.
- (11) Garcia-Echeverria, C.; Traxler, P.; Evans, D. B. ATP site-directed competitive and irreversible inhibitors of protein kinases. *Med. Res. Rev.* **2000**, *20*, 28–57.
- (12) Keserü, G. M. A virtual high throughput screen for high affinity cytochrome P450cam substrates. Implications for in silico prediction of drug metabolism. *J. Comput.-Aided Mol. Des.* **2001**, *15*, 649–657.
- (13) Schneider, G.; Böhm, H.-J. Virtual screening and fast automated docking methods. *DDT* **2002**, *7*, 64–70.
- (14) Kontoyianni, M.; McClellan, L. M.; Sokol, G. S. Evaluation of docking performance: Comparative data on docking algorithms. *J. Med. Chem.* **2004**, *47*, 558–565.
- (15) Charifson, P. S.; Corkery, J. J.; Murcko, M. A.; Walters, W. P. Consensus scoring: A method for obtaining improved hit rates from docking databases of three-dimensional structures into proteins. *J. Med. Chem.* **1999**, *42*, 5100–5109.
- (16) Wang, R.; Lu, Y.; Wang, S. Comparative evaluation of 11 scoring functions for molecular docking. *J. Med. Chem.* **2003**, *46*, 2287–2303.
- (17) Bissantz, C.; Folkers, G.; Rognan, D. Protein based virtual screening of chemical databases. 1. Evaluation of different docking/scoring combinations. *J. Med. Chem.* **2000**, *43*, 4759–4767.
- (18) *INSIGHT II*, 97 Molecular Modelling Program Package; Molecular Simulations (Accelrys) Inc.: San Diego, CA, 1997.
- (19) The 78 residues considered in the active site are Leu680, Leu683, Phe688, Lys692, Val693, Leu694, Gly695, Ser696, Gly697, Ala698, Phe699, Gly700, Thr701, Val702, Tyr703, Lys704, Gly705, Ile716, Pro717, Val718, Ala719, Ile720, Lys721, Glu722, Glu734, Ile735, Leu736, Glu738, Ala739, Val741, Met742, Ala743, Val750, Cys751, Arg752, Leu753, Leu754, Gly755, Ile756, Cys757, Val762, Gln763, Leu764, Ile765, Thr766, Glu767, Leu768, Met769, Pro770, Phe771, Cys773, Leu774, Leu775, Asp776, Tyr777, Val778, Arg779, Glu780, His781, His811, Asp813, Leu814, Ala815, Ala816, Arg817, Asn818, Val819, Leu820, Val821, Lys822, Thr823, Pro824, Lys828, Thr830, Asp831, Phe832, Gly833, and Leu834. The five water molecules are water2, water10, water11, water12, and water16.
- (20) Vema, A.; Panigrahi, S. K.; Rambabu, G.; Gopalakrishnan, B.; Sarma, J. A. R. P.; Desiraju, G. R. Design of EGFR kinase inhibitors: A ligand-based approach and its confirmation with structure-based studies. *Bioorg. Med. Chem.* **2003**, *11*, 4643–4653.
- (21) Rewcastle, G. W.; Denny, W. A.; Bridges, A. J.; Zhou, H.; Cody, D. R. Tyrosine kinase inhibitors. 5. Synthesis and structure–activity relationship for 4-[(phenylmethyl)amino]- and 4-(phenylamino)-quinazolines as potent adenosine 5'-triphosphate binding site inhibitors of the tyrosine kinase domain of the epidermal growth factor receptor. *J. Med. Chem.* **1995**, *38*, 3482–3487.
- (22) Bridges, A. J.; Zhou, H.; Cody, D. R.; Rewcastle, G. W.; McMichael, A.; Showalter, H. D. H.; Fry, D. W.; Kraker, A. J.; Denny, W. A. Tyrosine kinase inhibitors. 8. An unusually steep structure–activity relationship for analogues of 4-(3-bromoanilino)-6,7-dimethoxyquinazoline (PD 153035), a potent inhibitor of the epidermal growth factor receptor. *J. Med. Chem.* **1996**, *39*, 267–276.
- (23) Thompson, A. M.; Bridges, A. J.; Fry, D. W.; Kraker, A. J.; Denny, W. A. Tyrosine kinase inhibitors. 7. 7-Amino-4-(phenylamino)- and 7-amino-4-[(phenylmethyl)amino]pyrido[4,3-d]pyrimidines: A new class of inhibitors of the tyrosine kinase activity of the epidermal growth factor receptor. *J. Med. Chem.* **1995**, *38*, 3780–3788.
- (24) Rewcastle, G. W.; Palmer, B. D.; Thompson, A. M.; Bridges, A. J.; Cody, D. R.; Zhou, H.; Fry, D. W.; McMichael, A.; Denny, W. A. Tyrosine kinase inhibitors. 10. Isomeric 4-[(3-bromophenyl)amino]-pyrido[4,3-d]pyrimidines are potent ATP binding site inhibitors of the tyrosine kinase function of the epidermal growth factor receptor. *J. Med. Chem.* **1996**, *39*, 1823–1835.
- (25) Rewcastle, G. W.; Bridges, A. J.; Fry, D. W.; Rubin, J. R.; Denny, W. A. Tyrosine kinase inhibitors. 12. Synthesis and structure–activity relationships for 6-substituted 4-(phenylamino)pyrimido[5,4-d]pyrimidines designed as inhibitors of the epidermal growth factor receptor. *J. Med. Chem.* **1997**, *40*, 1820–1826.
- (26) Thompson, A. M.; Murray, D. K.; Elliott, W. L.; Fry, D. W.; Nelson, J. A.; Showalter, H. D. H.; Roberts, B. J.; Vincent, P. W.; Denny, W. A. Tyrosine kinase inhibitors. 13. Structure–activity relationships for soluble 7-substituted 4-[(3-bromophenyl)amino]pyrido[4,3-d]pyrimidines designed as inhibitors of the tyrosine kinase activity of the epidermal growth factor receptor. *J. Med. Chem.* **1997**, *40*, 3915–3925.
- (27) Fry, D. W.; Kraker, A. J.; McMichael, A.; Ambrosio, L. A.; Nelson, J. M.; Leopold, W. R.; Connors, R. W.; Bridges, A. J. A specific inhibitor of the epidermal growth factor receptor tyrosine kinase. *Science* **1994**, *265*, 1093–1095.
- (28) *Cerius² Molecular Modeling Program Package*; Molecular Simulations (Accelrys) Inc.: San Diego, CA.
- (29) *GOLD 2.0*; Cambridge Crystallographic Data Centre: Cambridge CB2 1EZ, UK.
- (30) Venkatachalam, C. M.; Jiang, X.; Oldfield, T.; Waldman, M. LiganFit: a novel method for the shape-directed rapid docking of ligands to protein active sites. *J. Mol. Graphics Modell.* **2003**, *21*, 289–307.
- (31) Cockerill, G. S.; Lackey, K. E. Small molecule inhibitors of the class 1 receptor tyrosine kinase family. *Curr. Top. Med. Chem.* **2002**, *2*, 1001–1010.
- (32) Kroemer, R. T.; Vulpetti, A.; McDonald, J. J.; Rohrer, D. C.; Trosset, J. Y.; Giordanetto, F.; Cotesta, S.; McMartin, C.; Kihlén, M.; Stouten, P. F. W. Assessment of docking poses: interactions-based accuracy classification (IBAC) versus crystal structure deviations. *J. Chem. Inf. Comput. Sci.* **2004**, *44*, 871–881.
- (33) We assume that water accepts a hydrogen bond from Thr766. See, Assefa H.; Kamath S.; Buolamwini J. K. 3D-QSAR and docking studies on 4-anilinoquinazolines and 4-anilinoquinoline epidermal growth factor receptor (EGFR) tyrosine kinase inhibitors. *J. Comput.-Aided Mol. Des.* **2003**, *17*, 475–493. If water were the donor and Thr766 an acceptor, the hydrogen bond geometry would not be so favorable, and the advantage of cooperativity would be lost. See Jeffrey, G. A. *An Introduction to Hydrogen Bonding*; Oxford University Press: Oxford, 1997; p 98.
- (34) Pierce, A. C.; Sandretto, K. L.; Bemis, G. W. Kinase inhibitors and the case for C–H···O hydrogen bonds in protein–ligand binding. *Proteins* **2002**, *49*, 567–576.
- (35) Desiraju, G. R.; Steiner, T. *The Weak Hydrogen Bond in Structural Chemistry and Biology*; Oxford University Press: Oxford, 1999.
- (36) Desiraju, G. R. Hydrogen bridges in crystal engineering: Interactions without borders. *Acc. Chem. Res.* **2002**, *35*, 565–573 and references cited therein.
- (37) For a general discussion of C–H···O versus other hydrogen bonds in protein–ligand structures, see Sarkhel, S.; Desiraju, G. R. *Proteins* **2004**, *54*, 247–259.
- (38) For difficulties in obtaining precise estimates of hydrogen bond distances from macromolecular crystal structures, the so-called crystallographic resolution problem, see ref 35, pp 345–346.
- (39) It may be noted that some of these compounds with a terminal morpholino group are similar to gefitinib.
- (40) The four ligands that do not improve after this treatment are **17**, **44**, **119**, and **127**.
- (41) In another satisfactory consensus model, 45 molecules were considered in the training set and 83 in the test set. Activity = $-0.3351 + 0.1263(\text{GOLDscore}) + 0.0087(\text{Dockscore}) + 0.0074(\text{Ludiscore}) - 0.00246(\text{vdWscore}) - 0.0041(\text{PLPscore})$; $r^2 = 0.861$, $r^2_{\text{cv}} = 0.81$, PRESS = 11.23, $r^2_{\text{bs}} = 0.86$. See the Supporting Information for the scatterplot.
- (42) Desiraju, G. R. Supramolecular synthons in crystal engineering—A new organic synthesis. *Angew Chem. Int. Ed. Engl.* **1995**, *34*, 2311–2327.

CI049676U